

Supplementary Material

DNA Hybridizing-Induced Fluorescence Variation in ThT: A New Strategy of Developing Aqueous Sensors for MO Genes

Yunkang Ma^a, Chenhui Wu^a, Wenjie Yang^a, Zhigang Gao^b, Lihua Chen^{a, b *}

^aKey Laboratory of Optic-electric Sensing and Analytical Chemistry for Life Science; Shandong Key Laboratory of Biochemical Analysis; Key Laboratory of Analytical Chemistry for Life Science in Universities of Shandong; Key Laboratory of Eco-chemical Engineering; College of Chemistry and Molecular Engineering, Qingdao University of Science and Technology, Qingdao 266042, PR China.

^bXinbao agricultural Science and Technology Development Co. Ltd., Wujiaqu, Xinjiang 831300, China

*Corresponding author: Lihua Chen, E-mail: lihuachen@qust.edu.cn.; Fax: +86 53284022681; Tel: +86 15054246089

Supporting information: Figure S1-S11 and Table S1-S4.

Experimental Section

1.1 Synthesis and Characterization of NH₂-MIL-53 (Al) (MOFs)

NH₂-MIL-53 (Al) (MOFs) were synthesized according to the previous reports¹. First, AlCl₃ 6 H₂O (0.78 g) and NH₂-BDC (0.56 g) were respectively dissolved in 7.5 ml deionized water and in 22.5 mL DMF, then poured into the PTFE bushing of the hydrothermal reaction kettle with a capacity of 100 mL and placed in the oven to react at 150°C for 24 h. After cooling, light yellow product was obtained by vacuum filtration. Next, it was dissolved in DMF and refluxed at 90°C for 8 h to remove residual water and unreacted ligands in the pores. Finally, the product was filtered and washed with acetone to obtain purified NH₂-MIL-53 (Al). The purified MOFs was diluted with deionized water to 20 mg mL⁻¹ and stored in a refrigerator at 4°C. If it is for long-term storage, the product will be placed in a vial filled with nitrogen and then placed in a dryer after the activation step. The purification step: the product was purified in boiling DMF for 5 hours in order to remove the remaining water molecules or unreacted ligands trapped in the pores. The activation step: the product was washed with acetone and dried in a vacuum oven at 30°C before further analysis.

1.2 Interaction of ThT/G4probe/target

Firstly, 10⁻⁶ M target was mixed with 10⁻⁶ M G4probe, then 25 mM, 50 mM, 75 mM and 100 mM K⁺ were respectively added into the above solution, then incubated for 2h. Finally, after the mixed operation with ThT (3 μM) for twenty minutes, the fluorescence signal was detected. Instead of 50 mM K⁺, Co²⁺, Te³⁺, Cu²⁺, Ca²⁺, Mg²⁺, Na⁺ and Al³⁺ (50 mM) were separately employed for the study of the influence of various ions on ThT/G4probe/target. In addition, organic small molecule (glucose, 5 mM, urea, 20 μg mL⁻¹ and ascorbic acid, 1 μg mL⁻¹), and a variety of proteins (DA, OMP31, BP26, BSA, 3 μg mL⁻¹) were used to study the interference to interaction of

ThT/G4probe/target.

Supporting Figures:**Table S1:** Comparison of different methods of MO detection.

Method	Concentration of sample	Concentration of detection	Pretreatment	Time
Microbial culture ^{2, 3}	Appropriate sample concentration-	Appropriate sample concentration	Yes	1-2 weeks
Isolation and immunological detection ⁴	Appropriate sample concentration	Appropriate sample concentration	Yes	More than 4 days
PCR ⁵	0.05 ng-100 ng	0.05 ng-100 ng	Yes	6-24 h
Real-Time RCR ⁶	2.2×10^2 to 2.2×10^7 genomes	2.2×10^4 copies	Yes	6-7 h
LAMP-LFD ⁷	1.0×10^2 CFU/mL	1.0×10^2 CFU/mL	Yes	1 h
This work	10^{-10} M- 10^{-6} M	10^{-10} M- 10^{-6} M	No	12 h

Table S2: Sequences of the oligonucleotides used in this study

Name	Sequence (5'→3')
G3Probe	CCATGC <u>CAAGGTGGAGTTCTTGCTGGTGAA</u> <u>ATTAGTGCATGGGTAGGGCGGG</u>
G4Probe	<u>AGGGTTAGGGTTAGGGTTAGGGTTCAAGGT</u> <u>GGAGTTCTTGCTGGTGAAATTAGT</u> CCCTAACCCCT
Target	ACTAATTCACCAGCAAGAACTCCACCTTG
M1	ACTAATGTCACCAGCAAGAACTCCACCTTG
M2	ACTAATGTCACCAGCAATAACTCCACCTTG
M3	ACTAATGTCACCAGCAATAACTCCACTTTG
WB	GACGGCCCTCTAGTAGGTCCTGTAGAACCA

G3Probe: The single underlined part is the G3 sequence (this sequence is from reference ⁸), and the double underlined part is the complementary sequence of target.

G4Probe: The single underlined part is the G4 sequence (Guanine (G)-rich DNA sequences which can form G-quadruplex structure. This sequence is from reference ⁹), and the double underlined part is the complementary sequence of target.

Sequences of the oligonucleotides that were used in this study was designed in a BLAST search of GenBank DNA sequences (<http://www.ncbi.nlm.nih.gov/Genbank/index.html>). And we found no homology with genes of other diseases.

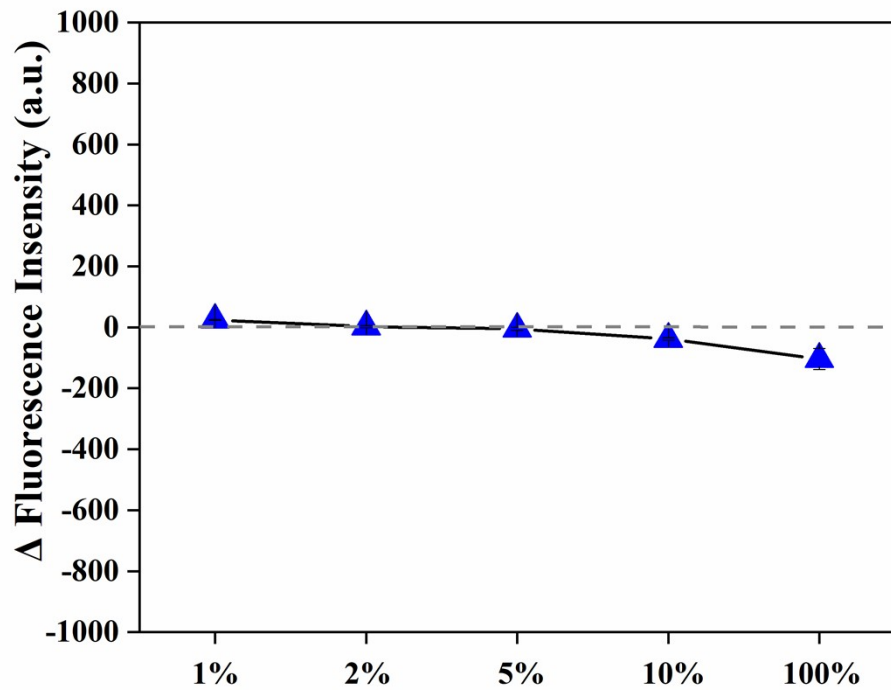


Fig. S1 Effects of different concentrations of urine on ThT fluorescence. The error bars represent the SD ($n = 3$).

ThT was directly added into the different concentrations of urine. The results demonstrated that no obvious fluorescence changes were observed before and after the addition of ThT (Fig. S1). It indicated that ThT as a desired candidate can be used in our new strategy.

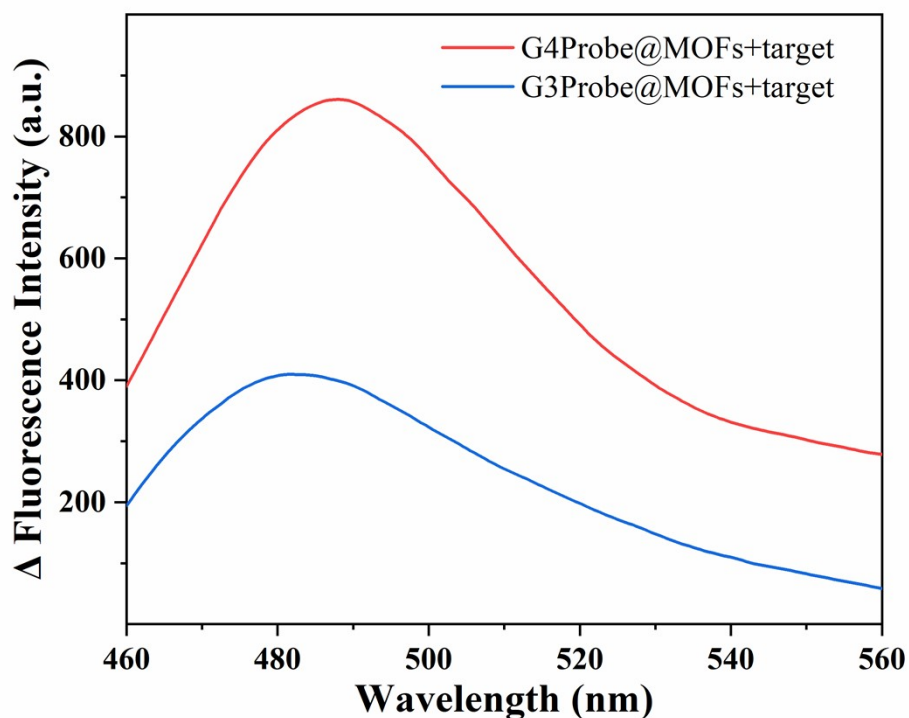


Fig. S2 Fluorescence intensity changes of ThT/G4probe/MOFs/target (red line) or ThT/G3probe/MOFs/target (blue line).

At the initial stage, G4 or G3 sequences reported in the literature was used as part of probe DNA. (Mohanty et al. 2013; Zhou et al. 2018b) After the hybridization experiment (Fig. S2), the effect of G4 is clearly better than that of G3. Therefore, G4 finally serves as the stem-loop structure of hairpin probe DNA. And the hairpin structure can also prevent the occurrence of intense fluorescence signal of ThT before the ring opening, which can further improve the accuracy of this strategy.

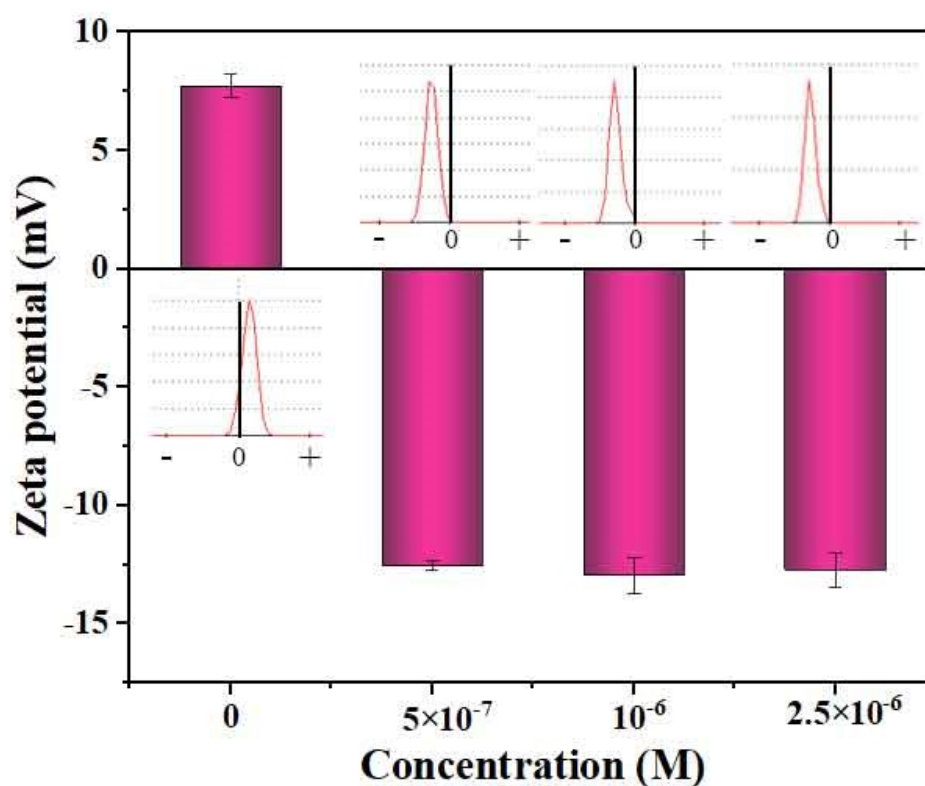


Fig. S3 Zeta potential of G4Probe/MOFs prepared under the different concentrations of G4Probe. (0 refers to MOFs only) The error bars represent the SD (n = 3).

Zeta potential analysis was carried out at room temperature, and each sample was measured three times in parallel. As can be seen from the Fig. S3, initially, the MOFs with amine groups showed a positive potential of +7.5 mV. With continuous adsorption of G4Probe into MOFs, Zeta potential gradually transits from positive to negative. When the DNA concentration increases to 10^{-6} M or higher, the zeta potential reaches -13 mV and remains basically unchanged. This indicated G4probe was saturated.

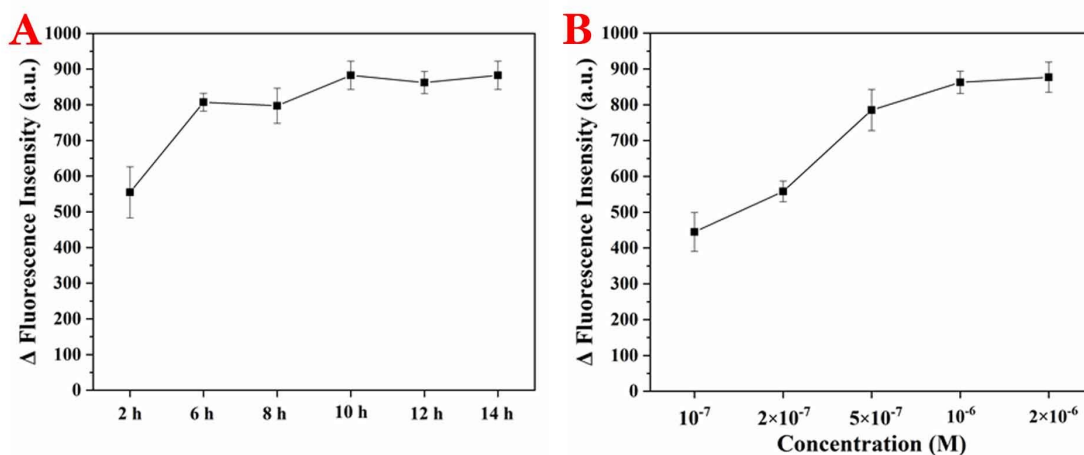


Fig. S4. The optimized adsorption time (A, from 2 h to 14 h, 37°C) and the optimized concentration (B, from 10^{-7} M to 2×10^{-6} M, 37°C) of G4Probe for the preparation of G4Probe/MOF. The error bars represent the SD (n = 3).

The adsorption time (from 2 h to 14 h) and the concentration of G4Probe (from 10^{-7} M to 2×10^{-6} M) were optimized during the preparation of G4Probe/MOFs. As can be seen from the Fig. S4A, Fig. S4B, the signal tends to be stable at 10 h to 14 h and G4Probe reaches saturation at 10^{-6} M, so the adsorption time is 12 h and the concentration of G4Probe is 10^{-6} M for the subsequent experiments.

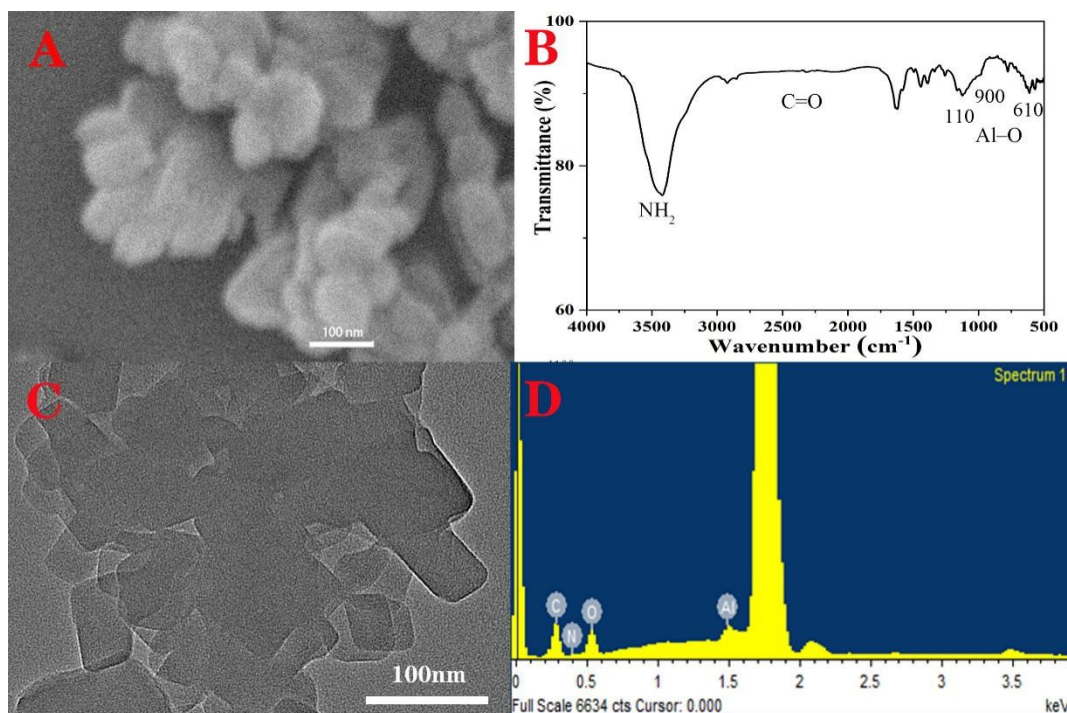


Fig. S5 SEM image (A), FTIR (B), TEM image (C), and EDS (D) of NH₂-MIL-53 (Al).

To confirm the successful synthesis of NH₂-MIL-53 (Al), a series of characterization was performed. First, the morphology of the synthesized compound was analyzed. Through scanning electron microscopy (Fig. S5A), it could be seen that the synthesized MOFs were rhomboid with an average particle size of about 90 nm. Subsequently, the IR spectrum of MOFs were studied. (Fig. S5B). The bands at 3417 cm⁻¹ and 3500 cm⁻¹ can be attributed to the symmetric and asymmetric stretching of amine group, the absorption bands at 1400 ~ 1600 cm⁻¹ to the symmetric and asymmetric stretching of carbonyl groups, the absorption peaks at ~1100 cm⁻¹, 900 cm⁻¹ and 610 cm⁻¹ to the Al-O vibration peak, an additional absorption peak at 1620 cm⁻¹ to the free DMF (Fig. S5C). Additionally, elements of C, N, O and Al were displayed in Energy dispersive spectroscopy (EDS) (Fig. S5D). All these indicate that NH₂-MIL-53 (Al) have been successfully synthesized.

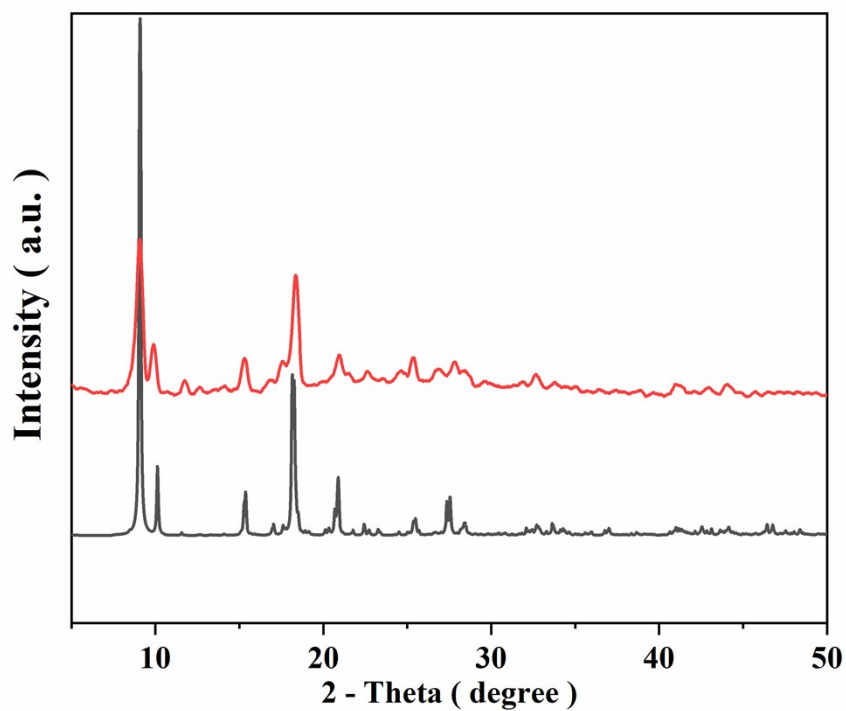


Fig. S6 The XRD patterns of simulated patterns of NH₂-MIL-53 (Al) (black) (CCDC 901254) and NH₂-MIL-53 (Al) (red).

The MOFs was analyzed by XRD. It can be seen from the Fig. S6 that the peak values at 2θ of 9.2° , 18.2° , 25.4° and 27.8° are basically consistent with the simulation results, indicating that the pure phase MOF is synthesized.

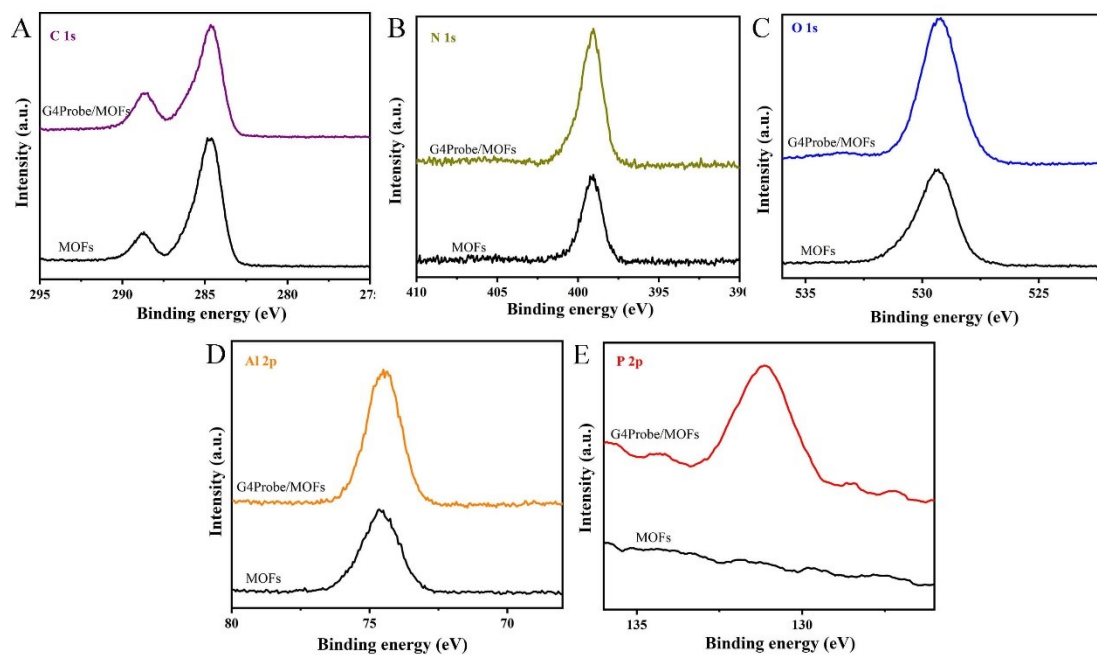


Fig. S7 XPS of C 1s (A), N 1s (B), O 1s (C), Al 2p (D) and P 2p (E) of MOFs and G4Probe/MOFs.

X-ray photoelectron spectroscopy (XPS) was utilized to survey the surface structure of the synthesized MOFs and G4Probe/MOFs and determine the elemental composition of MOFs and G4Probe/MOFs. For MOFs, Fig. S7 illustrates the survey spectra of the activated MOFs revealing the presence of C, N, O and Al as identified by their typical binding energies. For G4Probe/MOFs, the XPS analysis reveals the presence of P 2p peaks at the binding energy of 131.15 eV. This result indicates that the G4Probe are successfully loaded on NH₂-MIL-53 (Al) framework. The peak intensities and the mass percentages of the elements are tabulated in Table S3.

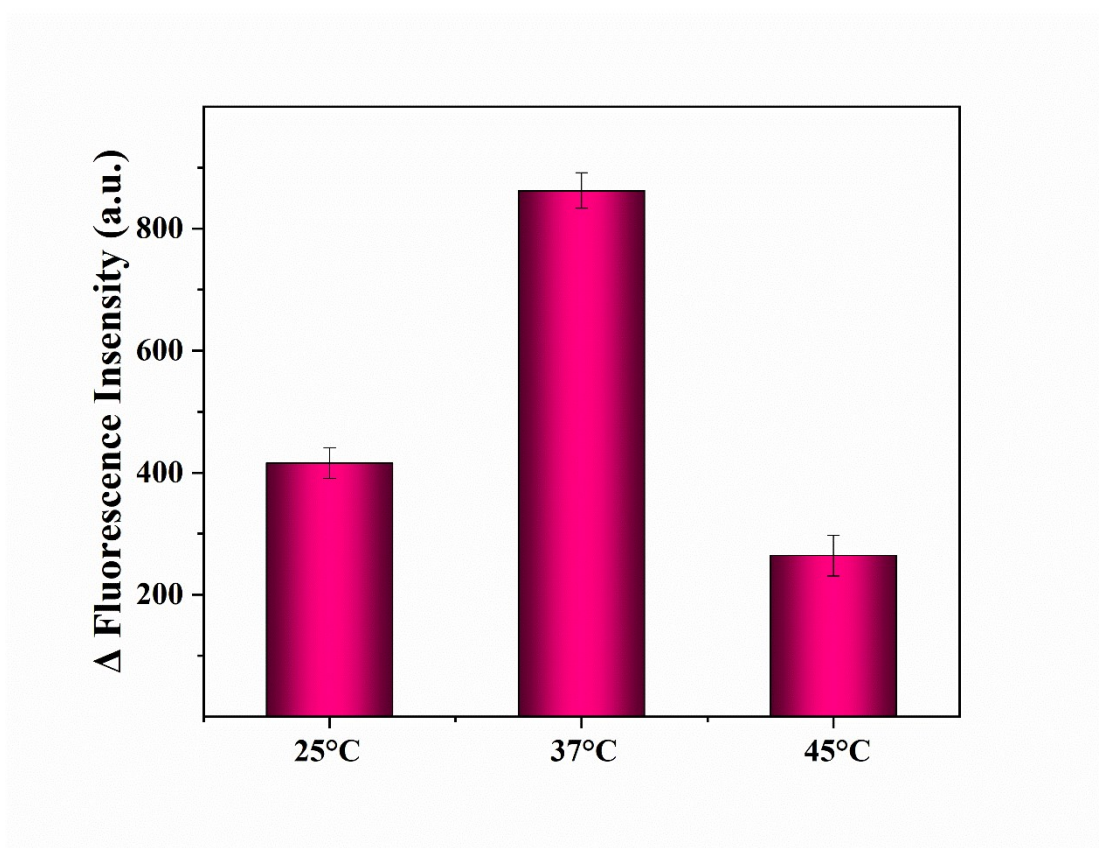


Fig. S8 Fluorescence intensity change of ThT/G4probe/MOFs/target under the different incubation temperatures varied from 25°C to 45°C. The error bars represent the SD (n = 3).

Here, 25°C, 37°C, 45°C are used in the study of the optimization of hybridization temperature, respectively. Fig. S8 shows that the fluorescence signal at 37°C is strongest and a sudden decrease at 45°C is observed due to the destabilization of G4 structures.

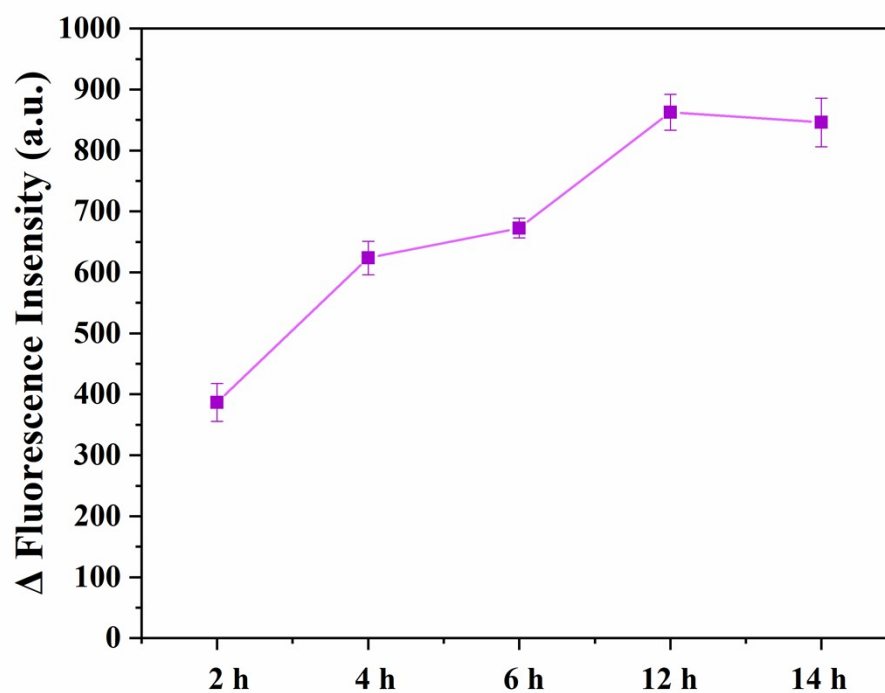


Fig. S9 Changes of fluorescence signal of ThT/G4probe/MOFs/target under the different incubation time varied from 2 h to 14 h. The error bars represent the SD (n = 3).

Here, 2 h, 4 h, 6 h, 12 h and 14 h are used in the study of the optimization of hybridization time, respectively. As showed in the Fig. S9, with the increase of hybridization time, the signal strength gradually increases, then reaches the maximum at 12 h.

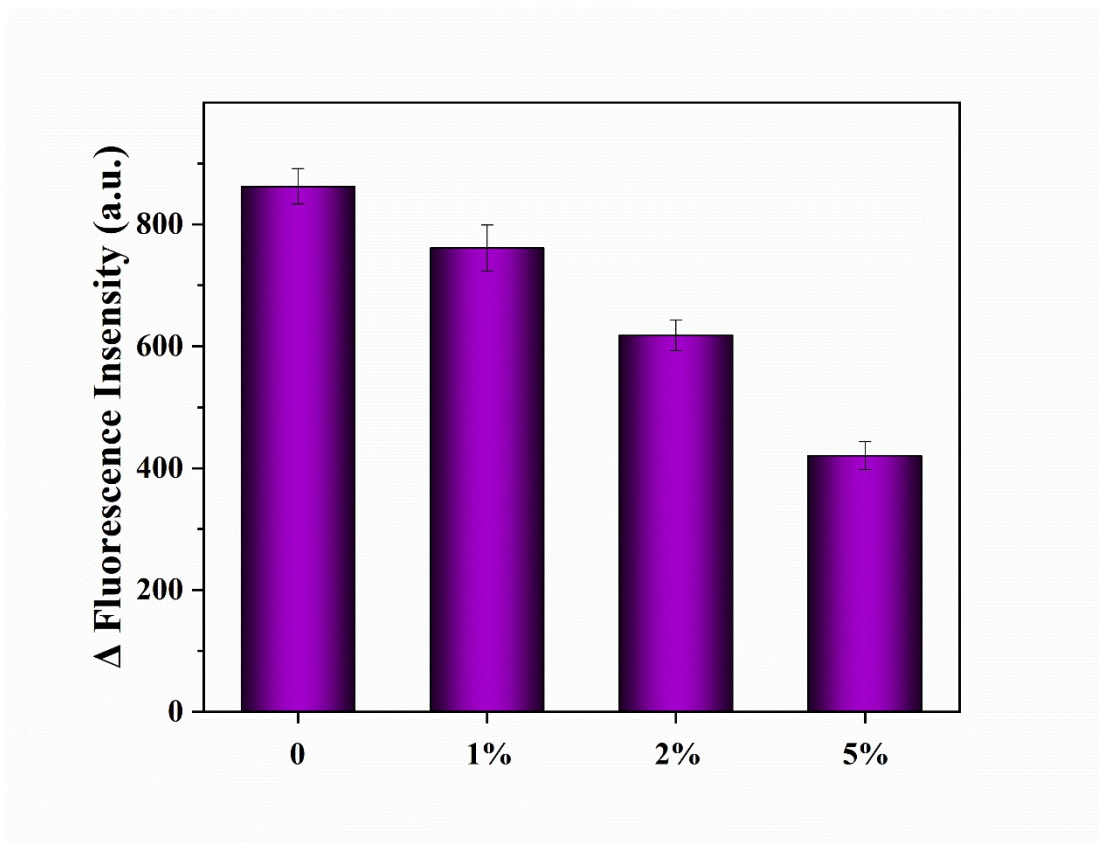


Fig. S10 Fluorescence intensity changes of ThT/G4probe/MOFs/target under the different concentration of urine. (0 refers to the buffer) The error bars represent the SD (n = 3).

1%, 2% and 5% diluted urine was used (Fig. S10) to study the real application ability of G4Probe/MOFs. Compared with the signal strength of ThT/G4Probe/MOFs/target in buffer, it is down only 9.1% in 1% diluted urine, which is in the acceptable range of sensitive detection.

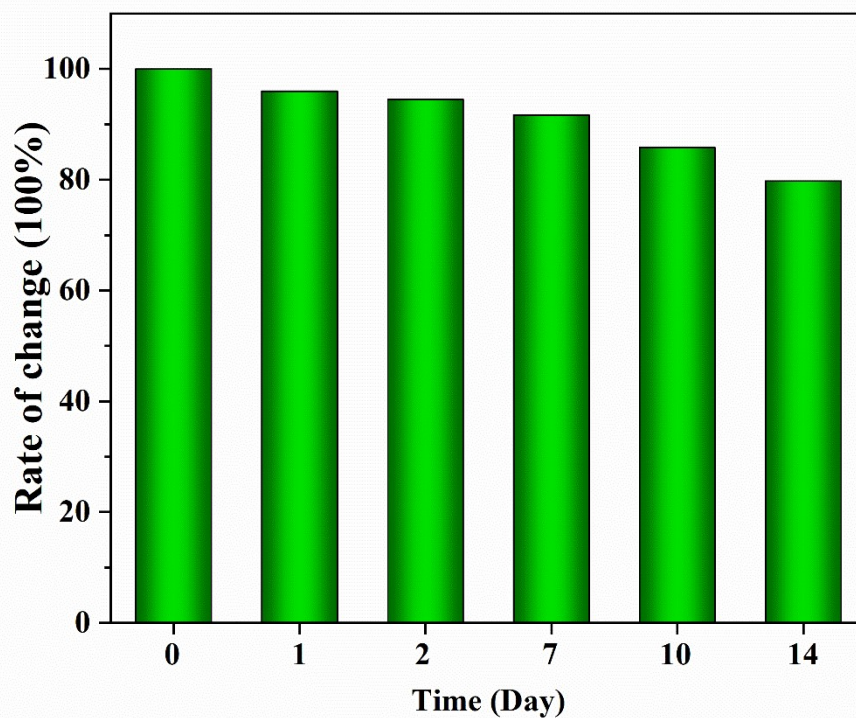


Fig. S11 Fluorescence response of ThT/G4Probe/MOFs/target after interval of 1 day, 2 days, 7 days, 10 days and 14 days at 4°C.

After an interval of 1 day, 2 days and 7 days, only about 4%, 5.5% and 8.3% degeneration in the fluorescence response were demonstrated respectively. However, the signal decreased 14.2% after 10 days and nearly 20% after 14 days (Fig. S11). This also means that the optimal application time is one week after the product is prepared.

Table S3: The peak binding energy and mass percentage of G4Probe/MOFs obtained through XPS.

Name	BE (eV)	Mass conc. (%)
P 2p	131.15	0.95
N 1s	396.45	4.68
Al 2p	71.90	14.16
C 1s	282.05	47.74
O 1s	529.20	32.47

Table S4: Application of MOFs-based strategies in the detection of various substances

Method	Material used	Detection target	Linear range	Limit of detection	media	Reference
Fluorescent detection	Ln-MOFs	DPA	0-100 μM	0.85 μM	In diluted serum	10
Fluorescent detection	g- CNQDs@ Zn-MOF	Riboflavin	0.005-1 μM	15 nM	In buffer	11
Fluorescent detection	MIL-88A	HIV	3-150 nM	1 nM	In buffer	12
Electrochemical detection	AuNPs/Cu-MOFs	A β	1 nM to 2 μM	0.45 nM	In buffer	13
Fluorescent detection	Ni-IRMOF-74-II	miRNA	1.25 to 100 nM	-	In buffer	14
Fluorescent detection	R6G/Eu-CdS@ZIF-8	DPA	0.1 to 150 μM	67 nM	In buffer	15
Fluorescent detection	MIPs	HAV	20-2500 pM	3 pM	In buffer	16
Fluorescent detection	NH ₂ -MIL-53(Al)	MO	10 ⁻¹⁰ M-10 ⁻⁶ M	23 pM	In diluted urine	this work

As you can see from the table S4, although metal organic frameworks (MOFs)-based sensor platform has been used in a broad range of clinical applications for pathogen biomarker detection due to their diverse structures and multifunctionalities, the complexity of clinical conditions with various biofoulants (proteins, polysaccharides and lipids) are still the major obstacle of this platform in quantitative analysis of disease markers. Ln-MOFs were used to detect DPA in diluted serum, but the linear range is narrow the detection limit was only 0.85 μM . This is not conducive

to its further application. This work shows not only a lower detection limit (23 pM) but also a wider linear range (from 10^{-10} M to 10^{-6} M) in buffer, even in % urine. Moving forward, direct testing in 100% urine will be necessary, where diluted biological environments have provided a starting point for new research avenues.

References

1. X. Cheng, A. Zhang, K. Hou, M. Liu, Y. Wang, C. Song, G. Zhang and X. Guo, Dalton Trans, 2013, 42, 13698-13705. <https://doi.org/10.1039/c3dt51322j>.
2. X. Wang, W. Zhang and Y. Hao, J Vet Sci, 2020, 21, e30. <https://doi.org/10.4142/jvs.2020.21.e30>.
3. H. Patel, D. Mackintosh, R. D. Ayling, R. A. Nicholas and M. D. Fielder, Vet Microbiol, 2008, 127, 309-314. <https://doi.org/10.1016/j.vetmic.2007.08.030>.
4. Y. C. Lin, R. J. Miles, R. A. Nicholas, D. P. Kelly and A. P. Wood, Res Vet Sci, 2008, 84, 367-373. <https://doi.org/10.1016/j.rvsc.2007.06.004>.
5. A. Daei, A. Khodakaram-Tafti, A. Derakhshandeh and M. J. I. J. o. V. R. Seyedin, 2020, 21.
6. F. Yang, X. Dao, A. Rodriguez-Palacios, X. Feng, C. Tang, X. Yang and H. Yue, J Vet Med Sci, 2014, 76, 1631-1634. <https://doi.org/10.1292/jvms.14-0094>.
7. J. Zhang, J. Cao, M. Zhu, M. Xu and F. Shi, World J Microbiol Biotechnol, 2019, 35, 31. <https://doi.org/10.1007/s11274-019-2601-5>.
8. H. Zhou, Z. F. Wu, Q. J. Han, H. M. Zhong, J. B. Peng, X. Li and X. L. Fan, Anal Chem, 2018, 90, 3220-3226. <https://doi.org/10.1021/acs.analchem.7b04666>.
9. J. Mohanty, N. Barooah, V. Dhamodharan, S. Harikrishna, P. I. Pradeepkumar and A. C. Bhasikuttan, J Am Chem Soc, 2013, 135, 367-376. <https://doi.org/10.1021/ja309588h>.
10. X.-B. Chen, C.-X. Qi, Y.-B. Xu, H. Li, L. Xu and B. Liu, Journal of Materials Chemistry C, 2020, 8, 17325-17335. <https://doi.org/10.1039/d0tc04001k>.

11. S. Feng, F. Pei, Y. Wu, J. Lv, Q. Hao, T. Yang, Z. Tong and W. Lei, *Spectrochimica Acta Part A: Molecular and Biomolecular Spectroscopy*, 2021, 246. <https://doi.org/10.1016/j.saa.2020.119004>.
12. H. Tan, G. Tang, Z. Wang, Q. Li, J. Gao and S. Wu, *Anal Chim Acta*, 2016, 940, 136-142. <https://doi.org/10.1016/j.aca.2016.08.024>.
13. Y. Zhou, C. Li, X. Li, X. Zhu, B. Ye and M. Xu, *Analytical Methods*, 2018, 10, 4430-4437. <https://doi.org/10.1039/c8ay00736e>.
14. S. Peng, M. Liu, B. Bie, Y. Zhang, H. Tang, Y. Sun and X. Zhou, *ACS Applied Bio Materials*, 2020, 3, 2604-2609. <https://doi.org/10.1021/acsabm.9b01189>.
15. X. Li, J. Luo, L. Deng, F. Ma and M. Yang, *Anal Chem*, 2020, 92, 7114-7122. <https://doi.org/10.1021/acs.analchem.0c00499>.
16. L. Wang, K. Liang, W. Feng, C. Chen, H. Gong and C. Cai, *Microchemical Journal*, 2021, 164. <https://doi.org/10.1016/j.microc.2021.106047>.